

Fragmentation of neutral C_n clusters ($n \leq 9$): experimental and theoretical investigations

G. Martinet¹, M. Chabot¹, K. Wohrer^{2,a}, S. Della Negra¹, D. Gardès¹, J.A. Scarpaci¹, P. Désesquelles¹, V. Lima¹, S. Díaz-Tendero³, M. Alcamí³, P.-A. Hervieux⁴, M.F. Politis², J. Hanssen⁴, and F. Martín^{3,b}

¹ Institut de Physique Nucléaire, Université Paris-Sud, 91406 Orsay Cedex, France

² GPS, Université Paris 6^c, 2 place Jussieu, 75251 Paris Cedex 05, France

³ Departamento de Química C-IX, Universidad Autónoma de Madrid, 28049 Madrid, Spain

⁴ LPMC, Institut de Physique, Technopôle 2000, 57078 Metz, France

Received 10 September 2002

Published online 3 July 2003 – © EDP Sciences, Società Italiana di Fisica, Springer-Verlag 2003

Abstract. We report on experimental and theoretical efforts designed to understand the fragmentation of small carbon clusters. Experimentally, a new detection system for high velocity fragments has been recently developed allowing the fragmentation of high velocity clusters to be totally recorded [1]. Results for the branching ratios of deexcitation of C_5 and C_9 formed by electron capture in high velocity C_5^+ , C_9^+ + He collisions are presented. Theoretically, the dissociation dynamics of C_5 has been investigated using a kinematical model based on the statistical theory of Weisskopf. In this model various structural quantities (geometries, dissociation energies, harmonic frequencies), are required for both the parent cluster and the fragments. They have been calculated within DFT and coupled-cluster formalisms for C_n up to $n = 9$. In all cases, a strong correlation between measured branching ratios and calculated dissociation energies is observed.

PACS. 36.40.Qv Stability and fragmentation of clusters

1 Introduction

Fragmentation is the most important deexcitation pathway of highly excited atomic clusters, still far from being as well understood as photon or electron emission in atoms. Indeed, cluster fragmentation is a complicated process that depends on many internal and external variables: cluster type, size, structure, temperature, etc. To analyse the effect of the latter, various theoretical approaches have been developed, in particular, statistical theories which are often used to interpret experimental data (see, for instance, [2–4]). In this paper, we present a joined experimental and theoretical effort aimed to test the statistical behaviour of fragmentation for neutral carbon clusters C_n . Experimentally, excited C_n clusters are produced by electron capture of high velocity (2.6 a.u.) C_n^+ projectiles in collisions with helium atoms. Their fragmentation, involving a large number of competing channels some of them with emission of several fragments, is totally recorded on an event by event basis by using a newly developed detection system [1]. Theoretically, we have adapted to the carbon case the sequential statistical evaporation model initially introduced for metal clusters [5]. For this purpose,

precise structure calculations have been carried out for C_n up to $n = 9$ using DFT and coupled-cluster formalisms. As a first test of the method, we have evaluated fragmentation branching ratios as functions of the internal energy for the C_5 cluster. The paper is organised as follows. In Section 2, the experimental setup and the principle of the fragmentation analysis are briefly recalled. In Section 3, a summary of the theoretical methods is given. All the results are presented and discussed in Section 4: experimental branching ratios for deexcitation of C_5 and C_9 , calculated dissociation energies for C_5 and C_9 , and calculated branching ratios for C_5 . Comparison between experiment and theory is discussed in detail. Finally, the conclusions and prospects of this work are given in Section 5.

2 Experimental methods

The experiments were done at the Tandem accelerator in Orsay with C_n^+ ionic carbon clusters ($n \leq 9$) of $2n$ MeV kinetic energy (constant velocity of 2.6 a.u.). The vibrational energy of the clusters is not known, but could be as large as 0.3 eV per vibrational mode, as explained in [6]. Most of the C_5^+ projectiles are expected to be linear [7]. The experimental set-up has been described previously [6]: it includes a collision chamber in which a gaseous

^a e-mail: wohrer@gps.jussieu.fr

^b e-mail: fernando.martin@uam.es

^c CNRS UMR 75088

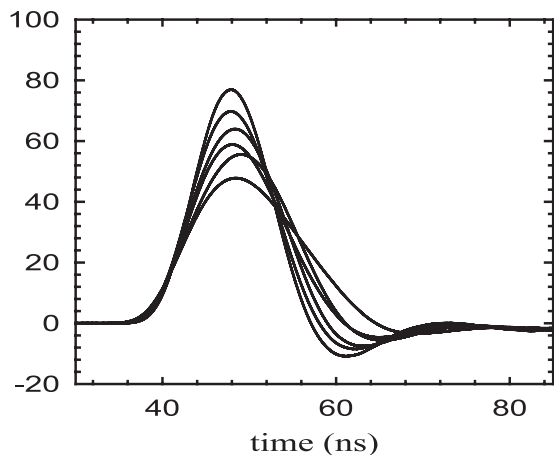


Fig. 1. Current signals for the six fragmentation channels of C_5 .

jet can be operated [8], an electrostatic deflector and a detection chamber equipped with several semiconductor detectors. The semi-conductor detector placed along the beam direction received undeflected neutral $\{C_n\}$ species resulting from electron capture by C_n^+ and undeflected neutral $\{C_p\}$ species ($p < n$) resulting from dissociative excitation and ionization of C_n^+ . Since the collision is very fast (10^{-16} s), neutral clusters formed by electron capture are likely to be in the conformation of incident C_n^+ . This implies, for instance, that C_5 clusters will be in a linear configuration. The distribution of final electronic states is not yet known. The distance between the jet and the detector of neutrals has been varied between 30 cm and 150 cm. Results presented below have been obtained for $L = 105$ cm corresponding to a flight time of 185 ns for the neutrals before detection. For the analysis of electron capture, dominantly dissociative [6], we have developed a new tool based on the shape analysis of current pulses delivered by the semiconductor detector. All details about this new method have been published recently [1]. The main result is that a fragmentation channel, characterised by a given combination of emitted fragments (for instance $C_n \rightarrow C_p/C_q/C_r$ with $p+q+r = n$), gives rise to a unique current shape which may be recognised as resulting from the sum of currents due to incident C_p , C_q and C_r clusters that are measured in the experiment. As an illustration we show in Figure 1 the current signals associated to the six fragmentation channels of C_5 . Thus, the fragmentation state of each event is deduced and, by working on large statistics, branching ratios are derived.

3 Theoretical methods

For a given total internal energy, the evaporation rate constants have been evaluated in the framework of the microscopic and microcanonical statistical theory of Weisskopf as introduced by Hervieux *et al.* in [5]. The basic ingredients of this theory are the dissociation energies and the

density of states of the different fragments. The density of states have been evaluated in the framework of the harmonic approximation, which requires the knowledge of the harmonic vibrational frequencies for all fragments. Rotational effects have been neglected.

To obtain the necessary information for the calculation of the rate constants we have optimised the geometries of the different species under consideration at the DFT-B3LYP level of theory [9,10] using a 6-311+G(3df) basis set. Harmonic vibrational frequencies have been obtained at the same level of theory. We will only report here on results with linear isomers. Indeed, starting from a linear C_n cluster (which, as explained above, is experimentally justified for C_5), we also expect fragments to be linear as well since sequential evaporation is likely to occur more rapidly than the time needed by the fragments to reorganise their internal structure. It has to be noted, however, that the global energy minima for C_4 , C_6 , and C_8 correspond to cyclic structures, as shown by high level geometry optimisations at the CCSD(T) level [12].

In order to test the accuracy of the DFT calculations, we have evaluated both absolute energies and dissociation energies of the smaller C_n clusters ($n \leq 5$) at the CCSD(T)/6-311+G(3df) level [11] using the DFT geometry. For dissociation energies, we have considered the spin multiplicity corresponding to the most stable state at the CCSD(T) level. As it can be seen in Table 1 the energies differ by less than 1 eV and the same energy order is predicted for the different channels. Our CCSD(T) results typically differ by less than 0.2 eV with those reported previously by Martin and Taylor using CCSD(T) optimised geometries [12]. It is also known that DFT calculations can present, for carbon clusters, important stability problems [13]. For this reason we have also performed stability tests to look for possible pathologies of the DFT method and we have found that, only in the case of $C_2(^1\Sigma_g^+)$ and $C_4(^1\Sigma_g^+)$, the DFT calculation is unstable with respect to a RHF \rightarrow UHF transformations [14]. It is in these cases where consideration of B3LYP energies instead of the CCSD(T) ones may lead to important errors. All these calculations have been performed by using the Gaussian-98 program [15].

4 Results and discussion

The measured branching ratios are reported in Table 1 for deexcitation of C_5 formed by electron capture in $C_5^+ + \text{He}$ collisions. Reported in this table are the measured branching ratios for the seven possible deexcitation channels and the associated error bars, of statistical nature only, since no ambiguity in the identification of the signals arose amongst the 800 analysed. In addition to these experimental data we report in the two last columns the dissociation energies calculated by DFT and coupled-cluster methods corresponding to transitions between the linear isomers. Examination of measured branching ratios reveals that, apart from a small fraction of intact clusters, most of the capture is dissociative, with dissociation into

Table 1. Measured branching ratios for deexcitation of C_5 and calculated energies D_e . ^aFirst value corresponds to the CCSD(T) calculation using B3LYP geometry. Number in parenthesis are results from reference [12] (CCSD(T)/cc-pVQZ calculation using a geometry fully optimised at CCSD(T)/cc-pVDZ level).

number of emitted fragments	Deexcitation channel	Measured branching ratio (error)	De(eV) B3LYP	De (eV) CCSD(T) ^a
1	C_5	0.16(± 0.02)		
2	C_3/C_2	0.59(± 0.04)	6.38	5.81(5.88)
	C_4/C	0.08(± 0.01)	7.13	7.48(7.13)
3	$C_3/C/C$	0.07(± 0.02)	12.46	11.79(11.95)
	$C_2/C_2/C$	0.07(± 0.01)	13.99	13.06(13.20)
4	$C_2/C/C/C$	0.025($\pm 8e^{-3}$)	20.07	19.05(19.27)
5	$C/C/C/C/C$	3e ⁻³ ($\pm 2e^{-3}$)	26.15	25.04(25.34)

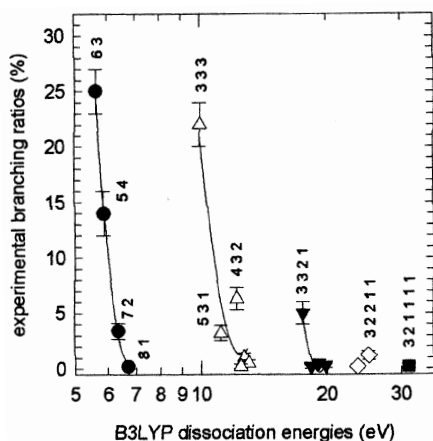


Fig. 2. Measured branching ratios of deexcitation of C_9 as a function of calculated dissociation energies. Black circles: two-fragments channels; open triangles: three-fragments channels; black triangles: four-fragments channels; open diamonds: five-fragments channels; black square: six-fragments channels. Solid lines are to guide the eye.

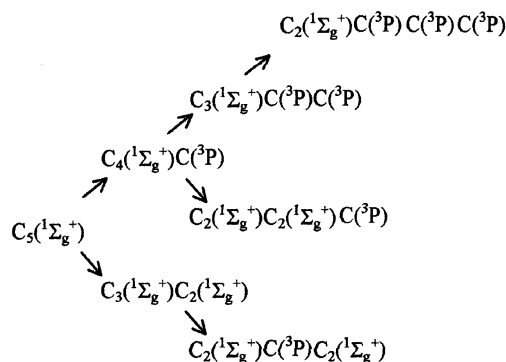
two fragments being largely dominant. Amongst the two-fragments break-up channels, the C_3/C_2 one is by far dominant which may be connected to the fact that the dissociation energy for this channel is lower than for the C_4/C channel.

The connection between measured branching ratios and calculated dissociation energies is striking in the case of the fragmentation of C_9 as shown in Figure 2. In this figure are reported calculated dissociation energies onto the X-axis and measured branching ratios onto the Y-axis. For C_9 , eighteen branching ratios over the thirty possible ones have been observed in the experiment.

It can be seen in Figure 2 that, channels with the lowest energy are those in which C_3 is emitted, which reflects the strong stability of this cluster. This stability was already deduced from photodissociation and collision induced dissociation experiments of low excited C_n^+ species long ago (see for instance [16–18]). Here the effects are magnified in the case of dissociation of highly excited neu-

trals: indeed amongst all dissociation channels of C_9 , the $C_3/C_3/C_3$ one has a remarkable large branching ratio. Also, within a group of channels associated to a given number of emitted fragments, a strong correlation exists between the magnitude of the branching ratio and the calculated dissociation energy. However, there are some clear exceptions to this rule, for instance the 5/3/1 channel as compared to the 4/3/2 one. This shows that the present energetic considerations are not sufficient to explain the observed branching ratios.

For this reason we have applied the sequential evaporation model of reference [5]. As an illustration, we have considered the case of C_5 , whose fragmentation chain is:



We start with C_5 in a linear configuration and, as mentioned above, we assume that the smaller fragments C_4 and C_3 are also produced in linear configurations. Rate constants for C and C_2 evaporations have been evaluated by using the dissociation energies from Table 1 and the B3LYP harmonic frequencies. These rate constants are used to build a system of differential equations that includes sequential evaporation events up to any order. Time integration is performed up to the value of the experimental TOF. This leads to branching ratios for the different fragmentation pathways.

We show in Figure 3 the corresponding fragmentation probabilities as functions of energy deposit. In order to compare these results with the experimental ones given in Table 1, one should convolute them with the experimental energy distribution of the parent cluster C_5 . This energy distribution depends on impact energy, but also on the initial cluster temperature. Although this energy distribution is unknown at present as discussed before, we can extract several interesting conclusions from Figure 3 alone. If we assume that the energy distribution is centered around 7 or 8 eV, one can see that the dominant channel is $C_3 + C_2$; this channel would be followed by C_5 and $C_4 + C$, which would contribute to the observed branching ratio through the lower and upper wings of the energy distribution. This is in agreement with the experimental results of Table 1. Similarly, the upper wing of the energy distribution may explain the observation of the $C_3 + C + C$ channel. Therefore, except for the $C_2/C_2/C$ channel (under further theoretical investigation), the present theoretical results are compatible with a cluster energy distribution centred around 7–8 eV.

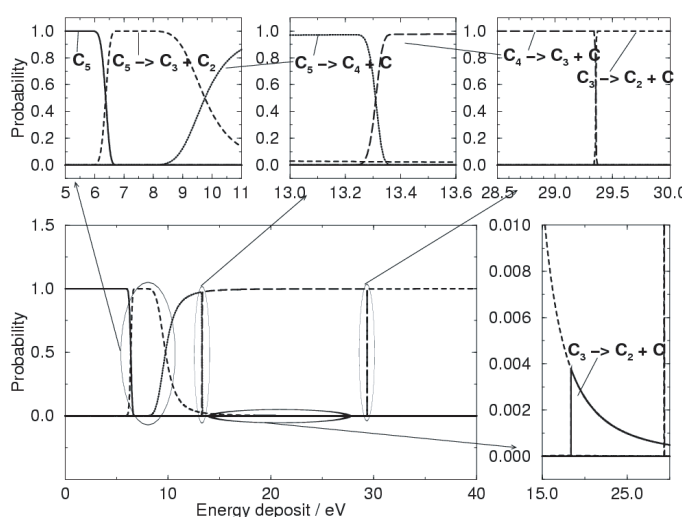


Fig. 3. Calculated fragmentation probabilities as functions of energy deposit.

It is worth stressing here that there does not always exist an energy distribution that is compatible with the experimental observations. For instance, we have found that, for C_4^+ (results to be published), an unreasonable choice of the geometries of the different fragments leads to branching ratios that are incompatible with the experimental observations for any choice of the cluster energy distribution.

5 Conclusions and perspectives

In conclusion, new results concerning the fragmentation of C_5 and C_9 neutral clusters have been presented, with measurements of all possible deexcitation channel branching ratios. A strong correlation between measured branching ratios and calculated dissociation energies has been observed, explaining the prominent branching ratios obtained for channels with C_3 emission. On the other hand, exceptions to this energetic rule have been observed indicating that other criteria must be considered. Theoretical calculations for deexcitation branching ratios of C_5 have been performed using a kinematical treatment based on the statistical theory of Weisskopf. In this treatment, energetic as well as entropic criteria are taken into account, which requires large scale structure calculations.

The latter have been performed using DFT and Coupled cluster formalisms. Theoretical calculations for the fragmentation branching ratios have been carried out using the experimental TOF (time of flight) of neutral fragments (180 ns), which is very important to expect agreement [5]. Theoretical predictions for C_5 are compatible with experimental observations on the basis of a cluster energy distribution centred around 7–8 eV. In the future, we intend to convolute the calculated branching ratios with a “reasonable” estimate of the energy distribution taking into account the initial cluster temperature and energy deposit in the capture process. Application of this model to larger clusters, such as C_9 presented here, will be also considered. We also plan to apply an alternative fragmentation model, such as Metropolis Monte Carlo [19], to compare with the present results.

References

1. M. Chabot *et al.*, Nucl. Instr. Meth. B **197**, 155 (2002)
2. E.E.E. Campbell, T. Raz, R.D. Levine, Chem. Phys. Lett. **253**, 261 (1996)
3. S. Matt, O. Echt, A. Stamatovic, J. Chem. Phys. **113**, 616 (2000)
4. C. Bréchnignac *et al.*, Chem. Phys. Lett. **335**, 34 (2001)
5. P.-A. Hervieux *et al.*, J. Phys. B **34**, 3331 (2001)
6. K. Wohrer *et al.*, J. Phys. B **33**, 4469 (2000)
7. M. Chabot *et al.*, Eur. Phys. J. D **14**, 5 (2001)
8. K. Wohrer, M. Chabot, R. Fossé, D. Gardès, Rev. Sci. Instrum. **71**, 2025 (2000)
9. C. Lee, W. Yang, R.G. Parr, Phys. Rev. B **37**, 785 (1988)
10. A.D. Becke, J. Chem. Phys. **98**, 5648 (1993)
11. R.J. Bartlett, G.D. Purvis, Int. J. Quant. Chem. **14**, 516 (1978)
12. J.M.L. Martin, P.R. Taylor, J. Chem. Phys. **102**, 8270 (1995); J.M.L. Martin, P.R. Taylor, J. Phys. Chem. **100**, 6047 (1996)
13. R. Bauernschmitt, R. Ahlrichs, J. Chem. Phys. **104**, 9047 (1996)
14. S. Díaz-Tendero, F. Martín, M. Alcamí, J. Phys. Chem. A **106**, 10782 (2002)
15. M.J. Frisch *et al.*, *Gaussian 98*, Revised A3 edn. (Gaussian, Inc.: Pittsburgh PA, 1999)
16. M.E. Geusic *et al.*, J. Chem. Phys. **84**, 2421 (1986)
17. S.W. McElvany, B.I. Dunlap, A. O’Keefe, J. Chem. Phys. **86**, 715 (1987)
18. C. Lifshitz, T. Peres, S. Kababia, I. Agranat, Int. J. Mass Spectrom. Ion Proc. **82**, 193 (1988); **93**, 149 (1989)
19. D.H.E. Gross, P.-A. Hervieux, Z. Phys. D **35**, 27 (1995)